Journal of Magnetics 3(2), 49-54 (1998)

Comparisons of Magnetic and Magneto-Optic Properties between Fe-rich and Nd-rich Amorphous Nd_XFe_{1-X} Alloys

Jai-Young Kim, Jeoung-Hoon Kim and Hyun-Woo Oh

Analytical Engineering Lab., Technology Consulting and Services Center, Samsung Advanced Institute of Technology, P.O. Box 111, Suwon, Kyunggi-Do, Korea

(Received 14 February 1998)

Dependence of magnetic and magneto-optic properties on composition of amorphous NdFe alloys has been studied to identify a promising magneto-optic recording material in the wavelength of a blue laser beam. From the view point of crystallographic state, perpendicular magnetic anisotropy energy and polar Kerr rotation angle, the Nd-rich region was found to be suitable for the research purpose.

1. Introduction

Recent commercial developments in a GaN blue laser diode [1-2] for high recording density of magneto-optic (MO) recording technology have strongly required suitable MO recording materials in the wavelengths of a blue laser beam. However, conventional MO recording materials for red laser beams ($\geq$635 nm), mainly based on amorphous heavy rare earth-transition metal (HRE-TM) alloys, such as amorphous TbFeCo alloys, show degradation of the polar Kerr rotation angle (θ_K) in the short blue laser wavelengths ($-$400 nm) [3], which results in the reduction of signal to noise ratio (SNR). Eventhough amorphous light rare earth - transition metal (LRE-TM) alloys show a large θ_K in the short wavelengths [4], these cannot apply to the MO recording materials, because of undesirable magnetic properties, including effective perpendicular magnetic anisotropy energy (PMAE). Tsutsumi *et al.* [5] and Suzuki *et al.* [6-8] fabricated amorphous NdFeTi, and NdFe, NdFeCo and PrFe alloys, respectively with positive intrinsic PMAE constants (K_U, which is defined as $K_{eff}+2\pi M_S^2$, where K_{eff} is the effective magnetic anisotropy energy obtained from a torque meter and M_S is the saturation magnetization) in the range of 10^6-10^7 ergs/cm^3. Furthermore, Gambino *et al.* [9-11] showed that the large substitution of LRE to HRE in amorphous LRE-HRE-TM alloys created effective PMAE constants (K_{eff}), but these revealed the decrease of θ_K in the short blue laser wavelengths, proportional to the substitutional amount of LRE to HRE.

Among amorphous RE-TM alloys, an amorphous Nd-TM alloy shows excellent θ_K in both the red and blue laser beams [12], which provides the wavelength-independent MO recording material. In this research, the magnetic and MO properties of amorphous NdFe alloys in term of Fe-rich and Nd-rich concentrations are reported.

2. Experimental Procedure

The amorphous Nd_XFe_{1-X} alloys were deposited on slide glass of 17 mm diameter and 10 mm thickness using a RF sputtering system under the basal pressure and Ar sputtering pressure of 3×10^{-7} and 8×10^{-3} mbar, respectively. The co-sputtering with different area of Fe masks on a Nd target was used to vary the concentration between Fe and Nd elements.

The concentration and film thickness, and crystallographic states of the amorphous Nd_XFe_{1-X} alloys were analyzed by a X-ray florence (XRF) and a X-ray diffractometer (XRD), respectively. A Scanning Electron Microscope (SEM) was used for the observation of surface morphology in the alloy films. Magnetic hysteresis loops parallel and perpendicular to the film plane were measured by a Vibrating Sample Magnetometer (VSM) up to 15 kOe. Spectral Kerr rotation angles from 400 nm to 800 nm were measured from a substrate-side by a Kerr spectrometer up to 10 kOe.

3. Results and Discussion

3.1 Structural investigation

Fig. 1 displays the X-ray diffraction curves of amorphous Nd_XFe_{1-X} alloys in terms of Nd concentration: (A) 13.4, (B) 14.2 (C) 17.3, (D) 38.2, (E) 40.5 and (F) 41. 3 at. % of Nd. In the Fe-rich region (A, B and C), crystalline peaks corresponding to 2θ=44.5° are observed. The intensities of the XRD peaks are reduced with the increase of Nd concentration and diffused at x=17.3.

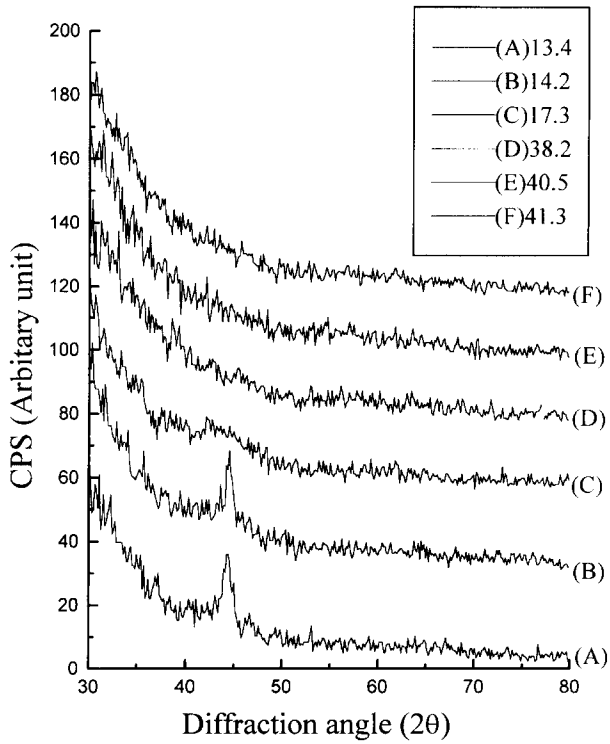

Fig. 1. X-ray diffraction curves of amorphous Nd_xFe_{1-x} alloys in terms of Nd concentration: (A) 13.4, (B) 14.2 (C) 17.3, (D) 38.2, (E) 40.5 and (F) 41.3 at. % of Nd.

However, no crystalline peak is observed in the Nd-rich region (D, E and F). Because the detected crystalline peaks are close to pure crystalline Fe peak (2θ=44.674°) [13], the precipitation of Fe element from the amorphous NdFe alloy matrix is expected in the Fe-rich region.

Fig. 2 (a), (b) and (c) present the surface morphologies of the amorphous Nd_xFe_{1-x} alloys in the Fe-rich region with x=13.4, 14.2 and 17.3, respectively observed by the SEM. As detected by the XRD curves in Fig. 1, the precipitated Fe particles in the range of μm order are observed from the NdFe alloy matrix, especially at x=13.4. As the Nd concentration increases, the particle sizes are reduced and hardly observed at x=17.3.

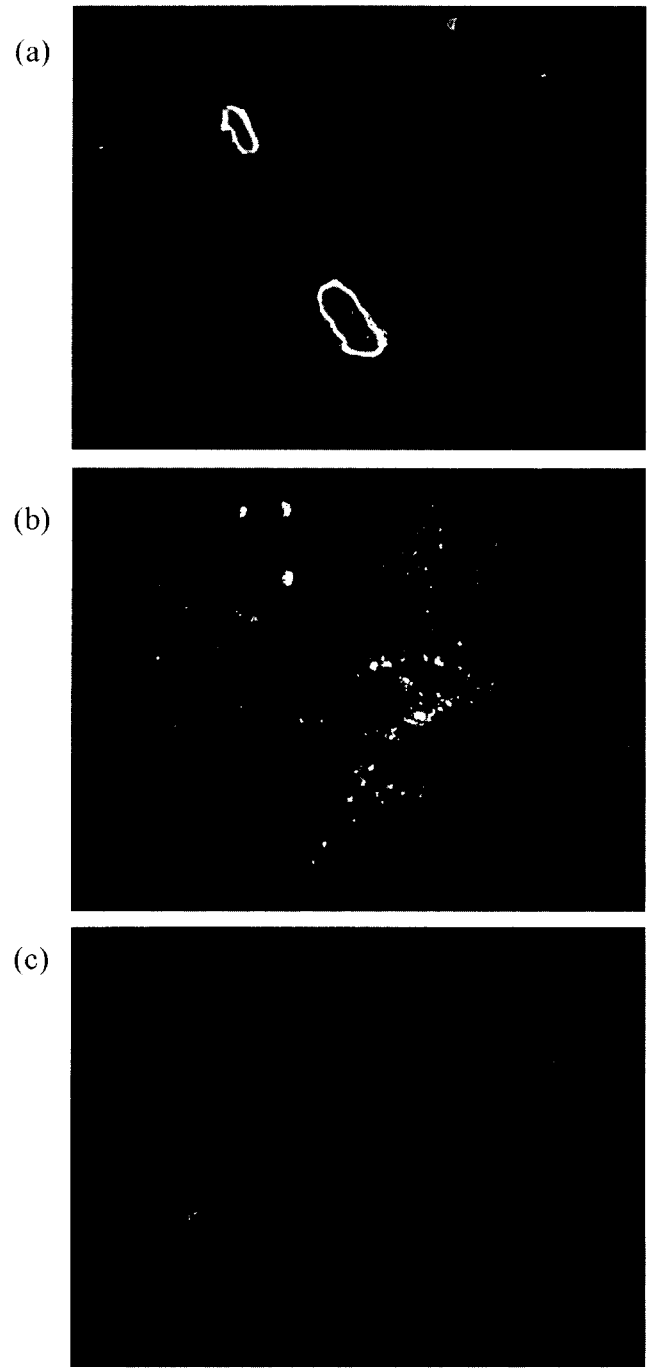

Fig. 2. (a), (b) and (c): Surface morphologies of the amorphous Nd_xFe_{1-x} alloys in Fe-rich regions with x=13.4, 14.2 and 17.3, respectively.

3.2 Magnetization

Fig. 3 (a), (b) and (c) show the magnetic hysteresis loops of amorphous Nd_xFe_{1-x} alloys in the Fe-rich region (13.4, 14.2 and 17.3 at. % of Nd, respectively), measured at room-temperature up to 15 kOe, and perpendicular (A) and parallel (B) to the film plane. The hysteresis loops display the preferential magnetic easy axis parallel to the film plane, even though an amorphous $Nd_{0.26}Fe_{0.74}$ alloy showed the easy axis preferentially perpendicular to the film plane below 200 K [14]. As the Nd concentration increases, perpendicular magnetic (PEM) hysteresis loops close to the parallel magnetic (PAM) hysteresis loops, which indicates the enhancement of PMAE. This is closely related to the existence of the precipitated Fe particles were shown in Fig. 1 and Fig. 2. On the Fig. 3, the PEM loops are composed of two parts; one is hysteresis in low magnetic fields and the other is non-hysteresis in high fields. Since the former is not dominant in a high concentration of Nd, the hysteresis and non-hysteresis parts originate from the precipitated Fe element and amorphous NdFe alloy matrix, respectively. Because the saturation magnetization (M_S) of pure Fe element (1,714 emu/cm^3) [15] is larger than that of amorphous NdFe alloys (500-700 emu/cm^3) [16], magnetic easy axis perpendicular to the film plane is preferred with the

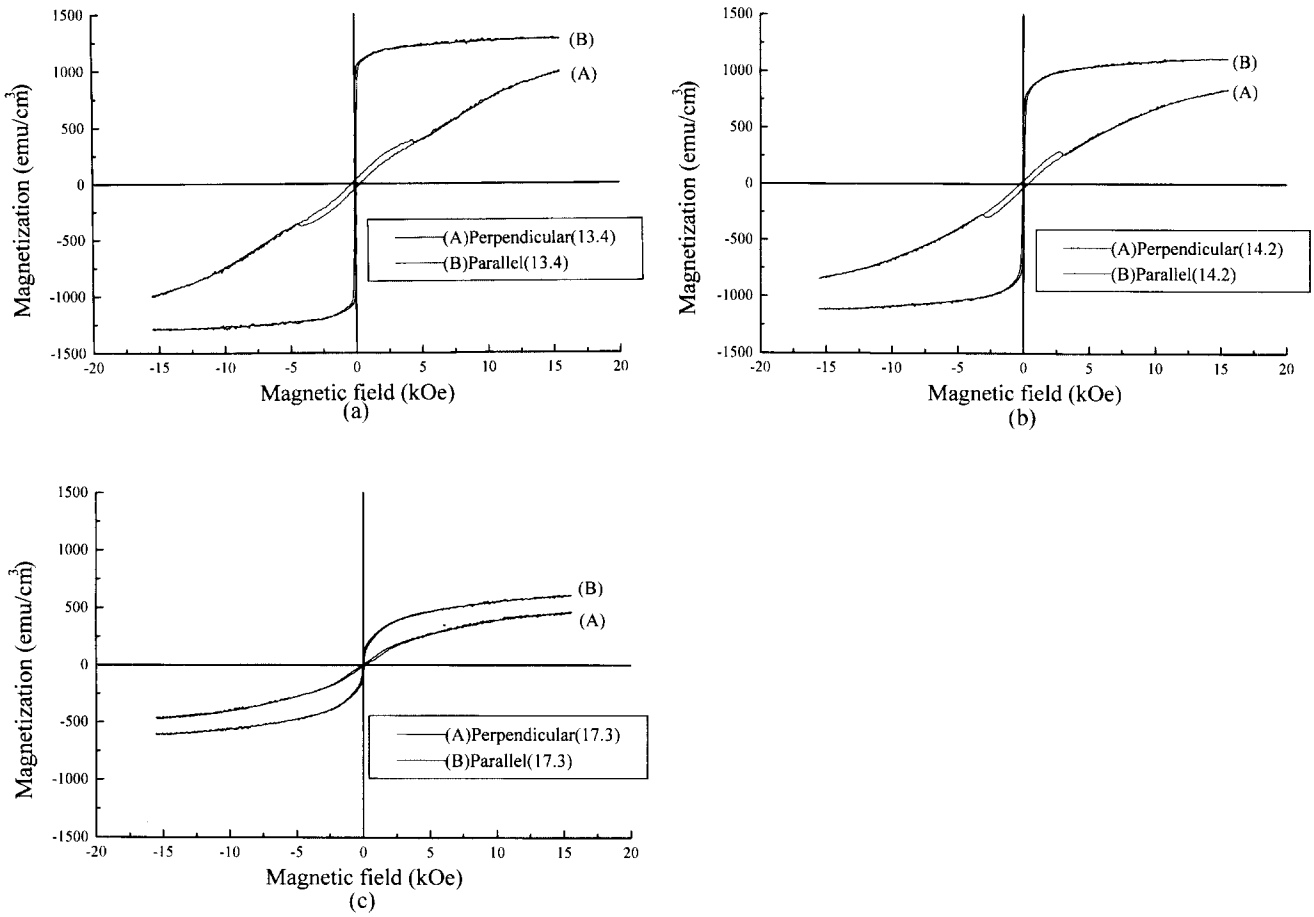

Fig. 3. (a), (b) and (c): Magnetic hysteresis loops of amorphous Nd_xFe_{1-x} alloys in the range of Fe-rich region (13.4, 14.2 and 17.3 at. % of Nd, respectively), measured at room-temperature up to 15 kOe, and perpendicular (A) and parallel (B) to the film plane.

increase of Nd concentration, due to the reduction of demagnetization energy. Since the increase of Nd concentration shows the preferential PMAE, investigation of magnetic process in Nd-rich region is necessary.

Fig. 4 (a), (b) and (c) show the magnetic hysteresis loops of amorphous Nd_xFe_{1-x} alloys in Nd-rich region (38.2, 40.5 and 41.3 at. % of Nd, respectively), measured at room-temperature up to 15 kOe, and perpendicular (A) and parallel (B) to the film plane. Because the deposited NdFe alloys in the Nd-rich region showed amorphous state without any precipitated Fe particle as shown in Fig. 1, the magnetic hysteresis loops hardly shows any dominant hysteresis loss, unlikely those in the Fe-rich region. PAM and PEM loops, compared with those in the Fe-rich region, are hard and easy, respectively to magnetize with respect to applied magnetic field, which means PMAE in the Nd-rich region is superior to that in the Fe-rich region. This is coincident with the previous Suzuki's result showing the maximum intrinsic PMAE (K_U) at 40 at.% of Nd concentration [8].

Fig. 5 displays the variation of magnetization at 15 kOe (M_{15}) in amorphous Nd_xFe_{1-x} alloys with respect to Nd concentration, measured at room-temperature perpendicular (closed circles) and parallel (open circles) to the film plane (dotted lines are guidelines for the eyes). As the Nd concentration increases, both the M_{15} in the Fe-rich and Nd-rich regions decrease. Since the asperomagnetic Nd subnet magnetic moment can be only saturated at extremely high magnetic field [17-18], it is clear that M_{15} is not a saturation value, as shown in Fig. 3 and Fig. 4. Taylor *et al.* [14] show that M_S of amorphous Nd_xFe_{1-x} alloys at 4.2 K decreases with the increase of Nd element. Hansen[19] also pointed out that compositional variation of M_S in amorphous NdFe alloys at 295 K is parabolic with the increase of M_S in Fe-rich region and inversely decrease of M_S in Nd-rich region. The variation in M_{15} in the Nd-rich region is consistent with Hansen' s result, but not in the Fe-rich region. This may be attributed to the existence of the precipitated Fe particles as pointed out in Fig. 3.

3.3 Coercive force and perpendicular magnetic anisotropy energy

Fig. 6 shows the changes of the coercive force (H_C) at 15 kOe in amorphous Nd_xFe_{1-x} alloys as a function of Nd concentration, measured at room-temperature parallel ($H_{C\parallel}$) and perpendicular ($H_{C\perp}$) to the film plane (dotted lines are

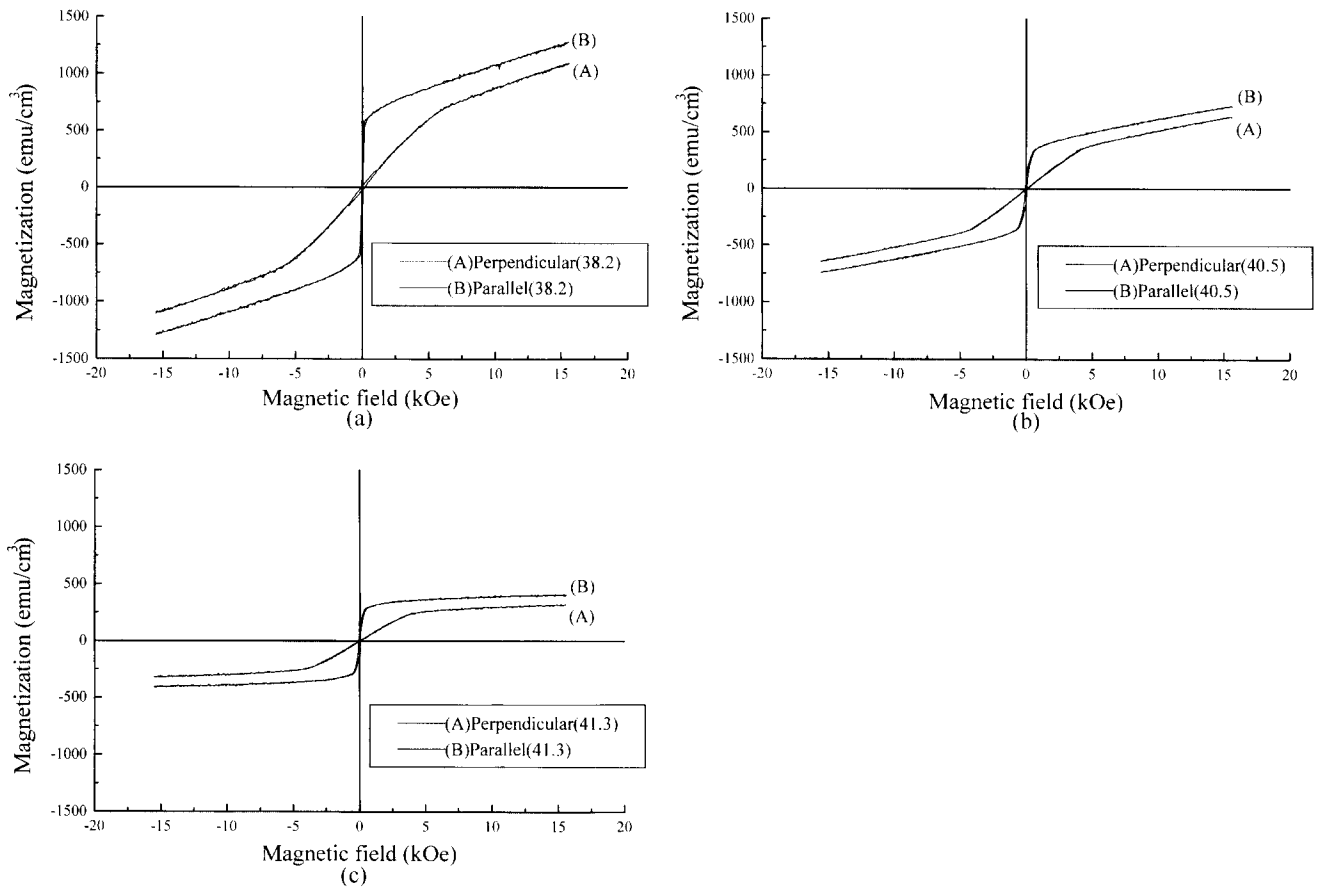

Fig. 4. (a), (b) and (c): Magnetic hysteresis loops of amorphous $NdXFe_{1-X}$ alloys in the range of Nd-rich region (38.2, 40.5 and 41.3 at. % of Nd), measured at room-temperature up to 15 kOe, and perpendicular (A) and parallel (B) to the film plane.

guidelines for the eyes). H_C of samples with Fe precipitate (x=13.4, 14.2 and 17.3 at%) with the show typical room-temperature coercive force of sputtered film about 300 Oe. As the Nd concentration increases, both of $H_{C\parallel}$ and $H_{C\perp}$ simultaneously decrease in the Fe-rich region, but $H_{C\parallel}$ and $H_{C\perp}$ increase and decrease, respectively in the Nd-rich region. Taylor *et al.* [14] showed the compositional variation of H_C at 4.2 K of an e-beam evaporated amorphous NdFe alloy as a parabolic shape. The different tendency in H_C between the two regions is related to that in magnetic anisotropy energy.

Fig. 7 (a) and (b) show the parallel (PAM) and perpendicular (PEM) magnetic hysteresis loops of amorphous Nd_XFe_{1-X} alloys in the Fe-rich and Nd-rich regions, respectively with respect to effective magnetic field. The effective magnetic field is calculated as follows,

$$H_{eff} = H_a - 4\pi N_d M \ (in\ cgs\ unit) \quad (1)$$

H_{eff}: Effective magnetic field (Oe)

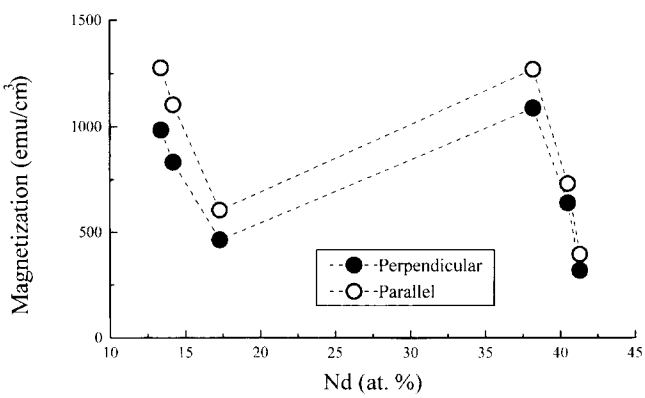

Fig. 5. Variation of room-temperature magnetization at 15 kOe (M_{15}) perpendicular and parallel to film plane in amorphous Nd_XFe_{1-X} alloys with respect to Nd concentration.

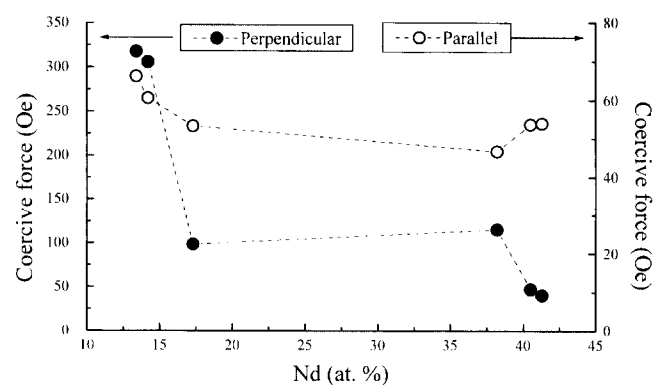

Fig. 6. Changes of coercive force (H_C) at 15 kOe in amorphous Nd_XFe_{1-X} alloys with respect to Nd concentration, measured at room-temperature perpendicular and parallel to film plane.

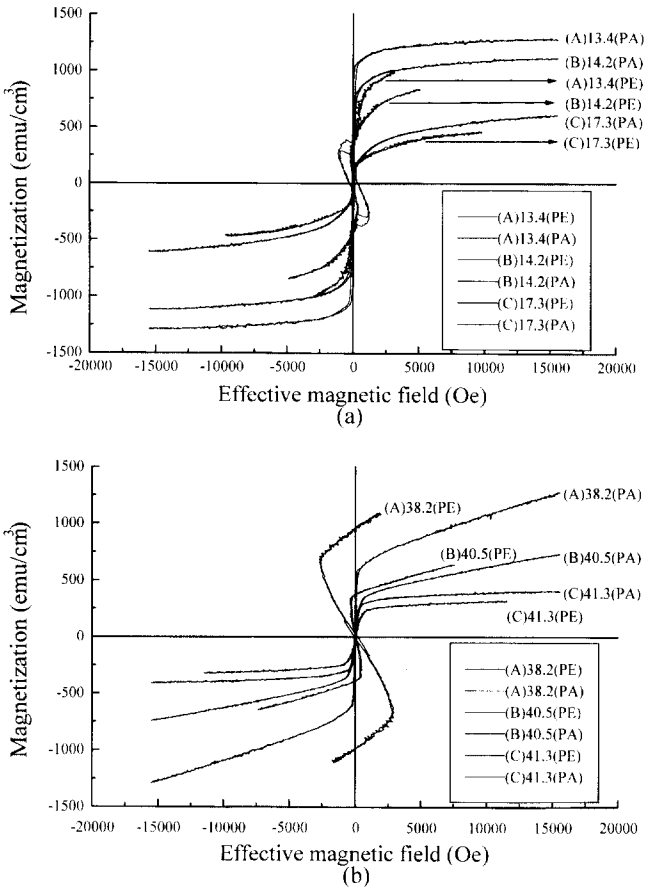

Fig. 7. (a) and (b): Magnetic hysteresis loops of amorphous Nd_xFe_{1-x} alloys in the Fe-rich and Nd-rich regions, respectively with respect to effective magnetic field.

H_a: Applied magnetic field (Oe)
N_d: Demagnetizing factor
M: Magnetization (emu/cm^3)

where, N_d is nearly 0 and 1 for PA and PE hysteresis loops, respectively for it depends mainly on the shape of the samples.

Magnetic anisotropy energy can be determined from the area associated with field-dependent magnetization curves measured parallel and perpendicular to the film plane by the following relationship,

$$K_U = \frac{1}{M_S} H_K \qquad (2)$$

K_U: Uniaxial magnetic anisotropy energy constant
H_K: Anisotropy field.

In the Fe-rich region, the PAM loops are easier to magnetize than PEM ones, which means in-plane magnetic anisotropy energy is reserved. As Nd concentration increases, the PEM loops are easy to magnetize, which can be qualitatively estimated from the reduction of the area between the PAM and PEM loops. But the PAM loops still show the preferential curves with respect to the effective magnetic field. Since addition of the Nd element is estimated to induce perpendicular anisotropy energy in this region. the further addition suggests the possibility of preferential PEM loops in the Nd-rich region.

In the Nd-rich region, PEM loops at x=38.2 and 40.5 show preferential magnetization process with respect to the effective magnetic field to PAM ones, which presents the existence of intrinsic perpendicular magnetic anisotropy energy in the Nd-rich region. As the Nd element further increases at x=41.3, the conversion of preferred magnetization process from PEM to PAM is occurred, which means the reduction in the perpendicular anisotropy energy. This may be attributed to the increase of magnetical ordering fluctuation in high Nd concentration.

3.4 polar Kerr rotation angle

Fig. 8 shows spectral dependence of the room-temperature polar Kerr rotation angles (θ_K) for amorphous Nd_xFe_{1-x} alloys, measured from the glass substrate-side. The amorphous NdFe alloys show the increase of θ_K toward the short wavelengths both Fe-rich and Nd-rich region. In the Fe -rich region with large Fe precipitations of x=13.4 and 14.2, θ_K changes its polarity from negative to positive around 700 nm. The negative θ_K of the Fe-rich region attributes to a large negative θ_K of Fe element [20]. Compared with θ_K in the Fe-rich region, compositional dependence of θ_K are constant in the Nd-rich region.

Fig. 9 shows the comparison of polar Kerr rotation angle (θ_K) at 400 nm with magnetization (M_{15}) perpendicular to the film plane, measured at room temperature. As Nd concentration increases in the Fe-rich, M_{15} decreases but θ_K increases. The decrease of M_{15} results from the reduction of the Fe precipitations which have a larger saturation magnetization than that of amorphous NdFe matrix [15-16]. The increase of θ_K in spite of the decrease of M_{15}, that is decrease of Fe precipitations, leads to the fact that the polarity of θ_K in Nd element possesses the opposite direction to that in Fe element, for the sign of θ_K is determined by the contribution of composed elements

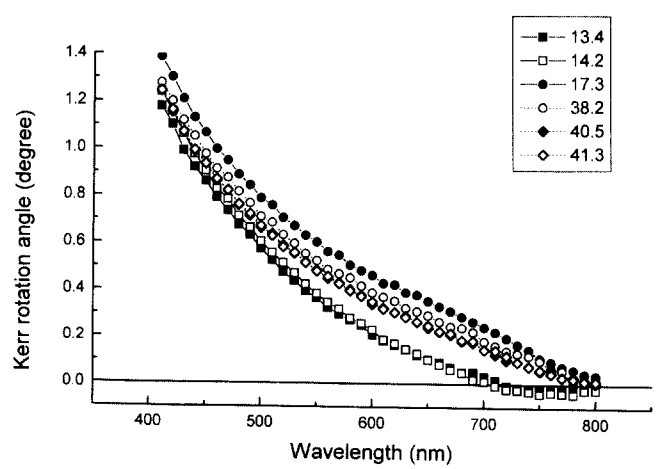

Fig. 8. Spectral dependence of the room-temperature polar Kerr rotation angles for amorphous Nd_xFe_{1-x} alloys.

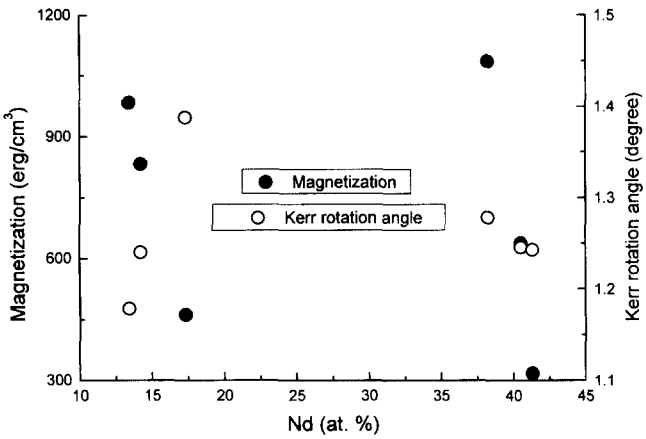

Fig. 9. Comparison of polar Kerr rotation angles at 400 nm with room-temperature magnetization at 15 kOe perpendicular to the film plane.

and the dominance of sub-magnetization in the magnetically saturated state. However, the positive θ_K in the Nd element is not coincident with McGuire *et al.*'s result [21], which reveals a negative θ_K for the light rate earth elements, Nd and Pr. In the Nd-rich region, both M_{15} and θ_K simultaneously decrease as the Nd increase. The reduction of θ_K may be originated from the decrease of magnetization and PMAE as discussed in Fig. 7(b).

4. Conclusions

The amorphous NdFe alloys in terms of Fe-rich and Nd-rich concentrations were deposited on slide glass substrates by R. F sputtering method. The precipitated Fe particles were observed in the Fe-rich region, which affect the magnetic and MO properties. Intrinsic in-plane and perpendicular magnetic anisotropy energy were obtained in Fe-rich and Nd-rich regions, respectively. The precipitated crystalline phase and in-plane anisotropy energy are not desirable factors for the MO recording material, due to the increase of noise level. The Nd-rich region in the NdFe alloy will be the promising MO recording material for the short wavelength of the blue laser beam, provided with the enhancements of magnetic properties.

References

[1] S. Nakamura, M. Senoh, S. Nagahama, N. Iwasa, T. Yamada, T. Matsushita, Y. Sugimoto and H. Kiyoku, Appl. Phys. Lett. **70** 1417 (1997).
[2] S. Nakamura, M. Senoh, S. Nagahama, N. Iwasa, T. Yamada, T. Matsushita, H. Kiyoku, Y. Sugimoto, T. Kozaki, H. Umemoto, M. Sano and K. Chocho, The second international conference on Nitride Semiconductors, Tokushima, Japan S1 444 (1997).
[3] T. Suzuki, C. J. Lin and A. E. Bell, IEEE Trans. Magn. MAG-24 2452 (1988).
[4] Y. J. Choe, S. Tsunashima, T. Katayama and S. Uchiyama, J. Magn. Soc. Jpn., 11 Suppl. 273 (1987).
[5] K. Tsutsumi and H. Sugahara, Jpn. J. Appl. Phys. **23**, L169-171 (1984).
[6] T. Suzuki, Jpn. J. Appl. Phys. **24**, L199-202 (1985).
[7] T. Suzuki, J. Magn. Magn. Mat. **50**, 265-271 (1985).
[8] T. Suzuki, A. Murakami and T. Katayama, IEEE Trans. MAG-23 2958 (1987).
[9] R. J. Gambino, T. S. Plaskett and R. R. Ruf, IEEE Trans. Magn. **24**, 2557 (1988).
[10] N. A. Bojarczuk, R. J. Gambino, T. S. Plaskett, P. Fumagalli and R. R. Ruf, J. Magn. Soc. Jpn. 17 Suppl. S1 48 (1993).
[11] W. Reim, R. J. Gambino, R. R. Ruf and T. S. Plaskett, J. Appl. Phys. **61**, 3349 (1987).
[12] P. Hansen, chapter 16, High density digital recording Ed. by K. H. J. Buschow, G. J. Long and F. Grandjean, Kluwer Academic Publishers 458 (1993).
[13] Swanson *et al.*, Natl. Bur. Stand. (U.S.), Circ. 539, IV 3 (1955).
[14] R. C. Taylor, T. R. McGuire, J. M. D. Coey and A. Gangulee, J. Appl. phys. **49**, 2885 (1978).
[15] American Institute of Physics Handbook, 2nd ed., New York, McGraw-Hill, (1963).
[16] Y. J. Choe, K. Nagase, S. Tsunashima and S. Uchiyama, Journal of the magnetic society of Japan, **21**, 207 (1988).
[17] K. Siratori, K. Nakayama, H. Ino, N. Sato and Y. Nakagawa, J. Magn. Magn. Mat. **83**, 341 (1990).
[18] H. Wan, C. P. Peng, R. Y. Fang and D. S. Dai, Phys. Rev. **B42**, 5067 (1990).
[19] P. Hansen, chapter 15, High density digital recording Ed. by K. H. J. Buschow, G. J. Long and F. Grandjean, Kluwer Academic Publishers 433 (1993).
[20] D. Weller and W. Reim, Mat. Res. Symp Proc. **232**, 71 (1991).
[21] T. R. McGuire and R. J. Gambino, J. Magn. Soc. Jpn. 11, Suppl. S1 261 (1987).